

Dynamic modelling of once-through subcritical steam generator for solar applications*

Asok Ray

Control and Flight Dynamics Division, The Charles Stark Draper Laboratory, Inc., Cambridge, Massachusetts, USA

(Received March 1980; revised June 1980)

This brief paper outlines a nonlinear dynamic model of a once-through subcritical steam generator for solar thermal plants. The purpose of the model is to describe the overall system performance and component interaction with sufficient accuracy for controller design, rather than to describe the microscopic details occurring within the steam generator. The model equations are arranged in state-space form to facilitate digital simulation and control system design. The modelling methodology is an extension of the earlier work of Ray and Bowman.

Introduction

The principal advantage of once-through steam generators over drum type units is lower capital cost. In this perspective, full scale solar thermal plants are likely to be of once-through type. For example, the DoE 10 MWe solar pilot plant to be built at Barstow, CA, is designed to have a once-through subcritical steam generator with throttle conditions at 510°C, $1.01 \times 10^7 \text{ N/m}^2$ (950°F, 1465 psia).¹ However, some manufacturers consider that forced recirculation drum-type steam generators are superior to once-through subcritical units for solar applications.²

The technology of solar thermal power generation is still at an early stage of development. Like fossil and nuclear plants, the process characteristics of solar plants are complex and interactive – they must be regulated by multi-variable control systems for safe and efficient operation. In addition, thermal-hydraulic dynamics of once-through steam generators are significantly complex; operating experience at fossil plants shows that once-through units are relatively more difficult to control.³ Design and development of commercial scale solar power plants cannot be accomplished by modification of existing fossil or nuclear plant parameters; *a priori* analytical studies are essential. Mathematical modelling and simulation have been proved to be useful analytical tools for investigating potential operational and control problems in large scale industrial processes as well as for control system design.⁴ Their application to solar thermal plants is very timely.

This brief paper presents the model equations for a once-through subcritical steam generator to be used as an element in overall system simulation and controller design of solar thermal plants. This model is not intended for studying microscopic thermal-hydraulic phenomena and flow maldistribution among the tubes. The modelling methodology is an extension of the earlier work of Ray and Bowman⁵ dealing with gas-cooled nuclear power plants. After some minor modifications, the methodology of reference 5 was successfully applied to model a 386 MWe oil-fired once-through subcritical unit. With the aid of the model, a controller was designed and implemented in the real plant resulting in improved performance.³

The modelling approach is described below. For brevity's sake the model equations which are identical to those in reference 5 have not been derived. However, a complete list of the equations that constitute the model are given in the Appendix, and the symbols are defined in the nomenclature.

Modelling approach

The purpose of the model is to describe overall system performance and component interaction with sufficient accuracy for controller design, rather than to describe the microscopic details occurring within the steam generator. If the model is a detailed representation of the process, computer runs for system simulation would be very costly, and the task of controller design too complicated.

The description of a solar pilot plant is given in Zonderman *et al.*¹ and the design details in Easton *et al.*⁶

* This work was done while the author was at Carnegie-Mellon University, Pittsburgh, PA, USA

The physical process of steam generation consists of distributed parameter dynamic elements, mathematically represented by nonlinear partial differential equations with space and time as independent variables. A lumped parameter approximation was used to formulate a finite-dimensional state-space model. Partial differential equations were reduced to a set of ordinary differential equations with time as the independent variable.

The model equations were formulated from: conservation relations for mass, momentum, and energy; semi-empirical relationships for fluid flow and heat transfer; and state relations for thermodynamic properties of water/steam. Major assumptions in addition to the lumped parameter approximation are: uniform fluid flow over pipe cross-sections; identical flow through each steam generator tube; and uniform incidence of heat flux on the steam generator tube surface from solar heliostats.

Development of model equations

A typical tube of a once-through subcritical steam generator was modelled in three lumped sections: compressed water (economizer); two-phase water (evaporator); and superheated steam (superheater) as shown in Figure 1. The length of each section was allowed to vary with time. A model solution diagram indicating the input and output variables is given in Figure 2.

The dynamic equations for water/steam flow are derived in reference 5 as equations (1) and (14); they are not repeated here. For energy storage in the tube walls, the temperature node in each section is considered at the external tube surface instead of the mean radius; otherwise, algebraic equations of fourth degree (due to radiative heat transfer) would have to be solved. Assuming the tube wall temperature to be constant in the evaporator section⁷ and linear with respect to tube length in the other sections, wall temperatures at section boundary (see Figure 1) are:

$$T_{m1} = 2T_{m2} - T_{m4} \quad (1)$$

$$T_{m3} = T_{m4} \quad (2)$$

$$T_{m5} = T_{m4} \quad (3)$$

$$T_{m7} = 2T_{m6} - T_{m4} \quad (4)$$

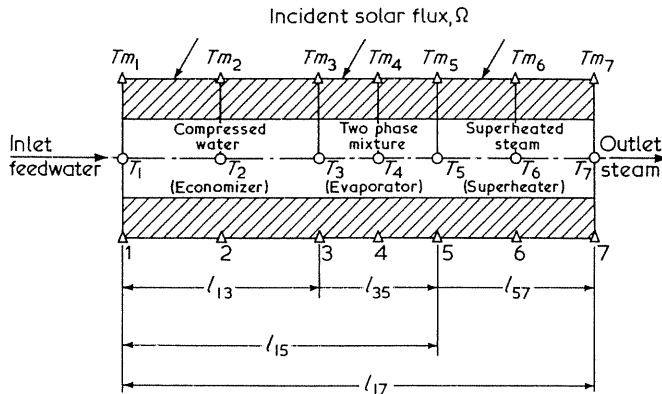


Figure 1 Schematic view of a steam generator tube with time varying phase boundaries. Node 1, feedwater entry; Node 2, average point for economizer; Node 3, economizer/evaporator boundary; Node 4, average point for evaporator; Node 5, evaporator/superheater boundary; Node 6, average point for superheater; Node 7, superheater outlet. (Δ), nodes for tube metal; (○), nodes for secondary coolant; T_m , tubewall temperature; T , water/steam temperature. Nodes 2-5 are time varying. Nodes 1 and 7 are fixed. l_{17} = steam generator tube length. $l_{17} = l_{13} + l_{35} + l_{57}$

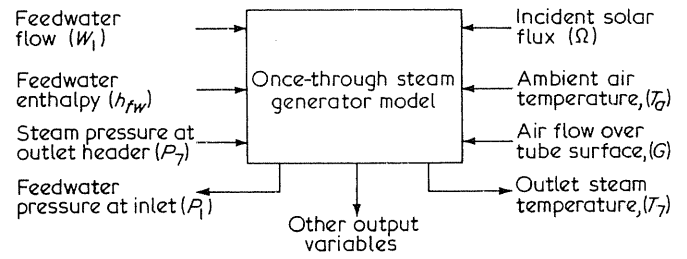


Figure 2 Model solution diagram. Arrows entering model are input variables; arrows leaving are output variables

The dynamic equations for energy storage in the tube wall are formulated in the time-varying control volumes of each section as shown:

Economizer

$$\frac{d}{dt}(C_m l_{13} T_{m2}) = Q_{g2} - Q_2 + C_m T_{m3} \frac{dl_{13}}{dt} \quad (5)$$

Rearranging equations (5) and (2):

$$\frac{dT_{m2}}{dt} = (Q_{g2} - Q_2)/(C_m l_{13}) + ((T_{m4} - T_{m2})/l_{13}) \frac{dl_{13}}{dt} \quad (6)$$

Evaporator

$$\begin{aligned} \frac{d}{dt}(C_m l_{35} T_{m4}) &= Q_{g4} - Q_4 \\ &+ C_m \left(T_{m5} \frac{dl_{15}}{dt} - T_{m3} \frac{dl_{13}}{dt} \right) \end{aligned} \quad (7)$$

Rearranging equations (7), (2) and (3):

$$\frac{dT_{m4}}{dt} = (Q_{g4} - Q_4)/(C_m l_{35}) \quad (8)$$

Superheater

$$\frac{d}{dt}(C_m l_{57} T_{m6}) = Q_{g6} - Q_6 - C_m T_{m5} \frac{dl_{15}}{dt} \quad (9)$$

Rearranging equations (9) and (3):

$$\begin{aligned} \frac{dT_{m6}}{dt} &= (Q_{g6} - Q_6)/(C_m l_{57}) \\ &+ ((T_{m6} - T_{m4})/l_{57}) \frac{dl_{15}}{dt} \end{aligned} \quad (10)$$

Equations (6), (8) and (10) are modified forms of equations (23), (24) and (25) in reference 5.

Heat transfer at the external surface of a typical tube consists of incident solar energy from a heliostat ensemble, and reradiation and convection losses from the tube surface to the environment. A model of the solar energy collector can be formulated on the basis of a specific heliostat system configuration. In this study, uniform solar energy flux was assumed as an input to the steam generator (see Figure 2). Surface areas per unit length of steam generator tube were taken as known parameters for incident solar energy, and radiation and convection losses.

Incident solar power on the steam generator tube is:

$$Q_s = A_s \Omega \quad (11)$$

Reradiation loss of power from a section of external tube surface to environment is averaged as:

$$Q_r = \sigma \epsilon A_r [(T_m + T_0)^4 - (T_a + T_0)^4] \quad (12)$$

Convective loss from tube surface is due to both natural and forced convection. Heat transfer due to turbulent natural convection is proportional to $(\Delta T)^{0.33}$ (see Holman⁸). On the other hand, forced convection is dependent on both magnitude and direction of flow over the tube surface. Air flow G over the tube under study was considered as a model input. Then, total convective losses from the tube surface are approximated as the algebraic sum of forced and natural convective losses:

$$Q_c = A_c l [K_{cf} G^{0.66} + K_{cn} (T_m - T_a)^{0.33}] (T_m - T_a) \quad (13)$$

For large values of G , natural convection loss is negligible in comparison to forced convection loss; whereas, for low values of G , forced convection is negligible.

Considering that a part β of the incident energy is reflected, the net rate of heat transfer at the external tube surface is:

$$Q_g = (1 - \beta) Q_s - Q_r - Q_c \quad (14)$$

which, for the three regions, are expressed as:

Economizer

$$\begin{aligned} Q_{g2} = & [A_s \Omega - \sigma \epsilon A_r ((T_{m1} + T_0)^4 \\ & + (T_{m3} + T_0)^4) / 2 - (T_a + T_0)^4] \\ & - A_c (K_{cf} G^{0.66} + K_{cn} (T_{m2} - T_a)^{0.33}) \\ & \times (T_{m2} - T_a) l_{13} \end{aligned} \quad (15)$$

Evaporator

$$\begin{aligned} Q_{g4} = & [A_s \Omega - \sigma \epsilon A_r ((T_{m3} + T_0)^4 \\ & + (T_{m5} + T_0)^4) / 2 - (T_a + T_0)^4] \\ & - A_c (K_{cf} G^{0.66} + K_{cn} (T_{m4} - T_a)^{0.33}) \\ & \times (T_{m4} - T_a) l_{35} \end{aligned} \quad (16)$$

Superheater

$$\begin{aligned} Q_{g6} = & [A_s \Omega - \sigma \epsilon A_r ((T_{m5} + T_0)^4 \\ & + (T_{m7} + T_0)^4) / 2 - (T_a + T_0)^4] \\ & - A_c (K_{cf} G^{0.66} + K_{cn} (T_{m6} - T_a)^{0.33}) \\ & \times (T_{m6} - T_a) l_{57} \end{aligned} \quad (17)$$

Equations (15)–(17), given above, replace equations (15)–(17) in reference 5.

Heat transfer from external tube surface to water/steam is due to conduction (in radial direction) through the tube wall and due to convection from the inner tube surface to the fluid. For single phase flow, convective heat transfer was computed by the Dittus and Boelter relation.⁸ For two-phase flow, the correlation of Levy (see Tong⁹) was used for nucleate boiling and correlation of Berlotti *et al.* (see Tong⁹) in partial film boiling region. These aspects are discussed, in detail, in reference 5. Heat transfer rates from the external tube surface to fluid for the three regions are:

Economizer

$$Q_2 = A_i l_{13} (T_{m2} - T_2) / (K_{mf2} W_1^{-0.8} + C_i) \quad (18)$$

where:

$$C_i = r_i \ln(r_o/r_i) / k_m$$

Evaporator

$$Q_4 = A_{i35} (T_{m4} - T_4) / (K_{mf4} + C_i) \quad (19)$$

Superheater

$$Q_6 = A_{i57} (T_{m6} - T_6) / (K_{mf6} W_7^{-0.88} + C_i) \quad (20)$$

Equations (18)–(20) are slightly modified forms of equations (18)–(20) in reference 5.

Thermal transport delay $\tau = A l_{13} \rho_2 / W_1$ due to water flow in the economizer was approximated by a first-order lag with $\tau/2$ as the time constant in reference 5. A better approximation can be obtained by Padé expansion (see Thaler and Pastel¹⁰). Using the Laplace transform notation, a second-order Padé expansion is:

$$\frac{h_1}{h_{fw}}(s) = \exp(-\tau s) = \frac{1 - \tau s/2 + (\tau s)^2/12}{1 + \tau s/2 + (\tau s)^2/12} \quad (21)$$

A state-space representation of equation (21) in the time domain is given as:

$$\frac{d\xi}{dt} = \eta - \frac{12}{\tau} h_{fw} \quad (22)$$

$$\frac{d\eta}{dt} = -\frac{12}{\tau^2} \xi - \frac{6}{\tau} \eta + \frac{72}{\tau^2} h_{fw} \quad (23)$$

$$h_1 = \xi + h_{fw} \quad (24)$$

In reference 5, the section on the primary coolant (covering equations (26)–(29)) is not applicable to solar thermal systems.

Model parameters

The model parameters were calculated from the design data and physical dimensions of a typical solar thermal plant, given in Table 1. For each region, water/steam temperature, section length, and tube wall temperature were calculated from energy balance. Pressure drop and spatial average density were obtained from fluid properties and friction factors; for two-phase pressure drop, the correlation of

Table 1 Design data and physical dimensions

Total number of steam generator tubes = 1314			
Dimensions of a steam generator tube			
length	$\begin{cases} 13.00 \text{ m} \\ 42.64 \text{ ft} \end{cases}$	I.D. $\begin{cases} 0.00683 \text{ m} \\ 0.269 \text{ in} \end{cases}$	O.D. $\begin{cases} 0.0127 \text{ m} \\ 0.5 \text{ in} \end{cases}$
Outlet steam pressure P_7 ,	$\begin{cases} 1.01 \times 10^7 \text{ N/m}^2 \\ 1465 \text{ psia} \end{cases}$	temperature T_7 ,	$\begin{cases} 510^\circ \text{ C} \\ 950^\circ \text{ F} \end{cases}$
Feedwater enthalpy at inlet h_1 ,	$\begin{cases} 1.219 \times 10^6 \text{ Joule/kg} \\ 523.48 \text{ BTU/lbm} \end{cases}$		
Normal air velocity G	$\begin{cases} 6.7 \text{ m/s} \\ 22 \text{ ft/s} \end{cases}$	ambient temperature T_a	$\begin{cases} 15.6^\circ \text{ C} \\ 60^\circ \text{ F} \end{cases}$
Normal solar flux Ω	$\begin{cases} 200 \text{ kW/m}^2 \\ 19.6 \text{ BTU}/(\text{ft}^2 \text{ s}) \end{cases}$		

Thom (see Collier⁷) was used. The averaging constants were obtained from steady-state values of the plant variables at inlet, outlet and spatial average points.

Results and discussion

The steady-state solutions of the model equations were obtained at four different levels of insolation for fixed throttle steam conditions at 510°C, $1.01 \times 10^7 \text{ N/m}^2$ (950°F, 1465 psia). The results are listed in Table 2. With the decrease in insolation, feedwater flow is accordingly reduced to maintain the throttle steam temperature. The lengths of economizer and evaporator monotonically decrease with reduction in insolation, and, therefore, the superheater length increases. Reduced insolation decreases radial heat flux in each section of tube wall resulting in significant changes in temperatures at the external tube surface.

The results of solar steam generator simulation are presented in Figures 3-6 in the form of a series of curves representing the dynamic response of four plant variables at 80% insolation. Each figure shows three responses of a particular plant variable to a 5% step decrease in solar flux Ω , a 5% step increase in feedwater flow W_1 , and a 5% step decrease in steam header pressure P_7 . In each case, the input variable under consideration was perturbed from its operating point keeping the other two held constant at their undisturbed value. The step disturbances were applied at time $t = 10$ s to display the steady state condition before initiation of the disturbances. Dynamic responses were observed for a period of 130 s.

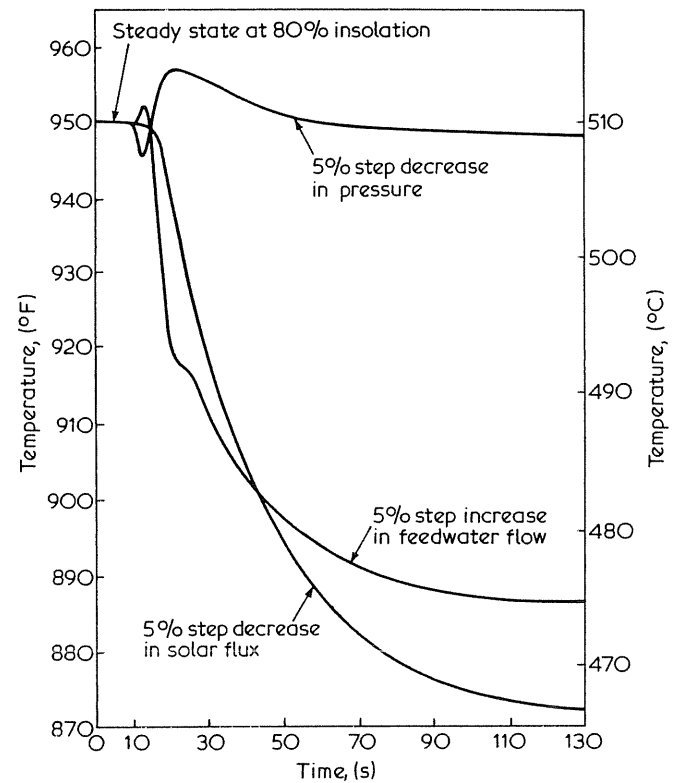


Figure 3 Superheater outlet steam temperature transients at 80% insolation

Table 2 Steady-state model performance for single steam generator tube

Process variables			% insolation			
			100	80	60	40
Water/steam flow per tube	W_1	kg/s	0.01864	0.01452	0.01041	0.00629
		lb/s	0.04109	0.03202	0.02295	0.01388
Steam flow to turbine	W_v	kg/s	24.493	19.081	13.676	8.270
		lb/s	53.992	42.074	30.156	18.238
Economizer length	l_{13}	m	1.190	1.181	1.171	1.144
		ft	3.900	3.870	3.840	3.750
Evaporator length	l_{35}	m	7.575	7.542	7.478	7.338
		ft	24.850	24.740	24.530	24.070
Superheater length	l_{57}	m	4.235	4.277	4.351	4.518
		ft	13.890	14.030	14.270	14.820
Economizer tube temperature	T_{m2}	°C	326.1	322.1	317.8	313.3
		°F	619.0	611.7	604.1	596.0
Evaporator tube temperature	T_{m4}	°C	340.6	334.7	328.8	322.9
		°F	645.0	634.4	623.8	613.2
Superheater tube temperature	T_{m6}	°C	453.8	447.7	440.8	432.2
		°F	848.9	837.9	825.4	809.9
Economizer heat flow	Q_2	kW	3.429	2.671	1.913	1.156
		BTU/s	3.620	2.820	2.020	1.220
Evaporator heat flow	Q_4	kW	21.749	16.947	12.144	7.341
		BTU/s	22.960	17.890	12.820	7.750
Superheater heat flow	Q_6	kW	11.501	8.961	6.423	3.884
		BTU/s	12.140	9.460	6.780	4.10
Total heat flow	$Q_2 + Q_4 + Q_6$	kW	36.679	28.579	20.480	12.381
		BTU/s	38.720	30.170	21.620	13.070

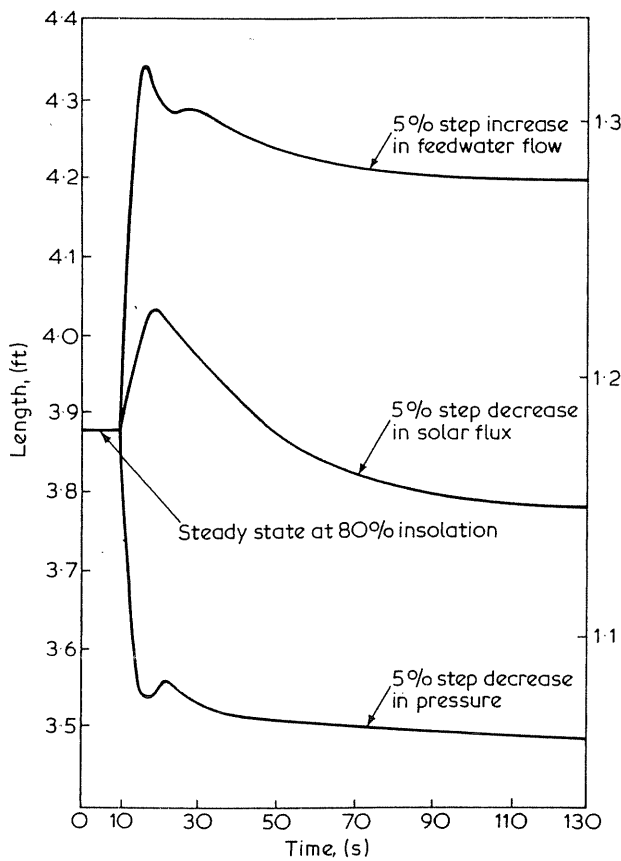


Figure 4 Economizer length transients at 80% insolation

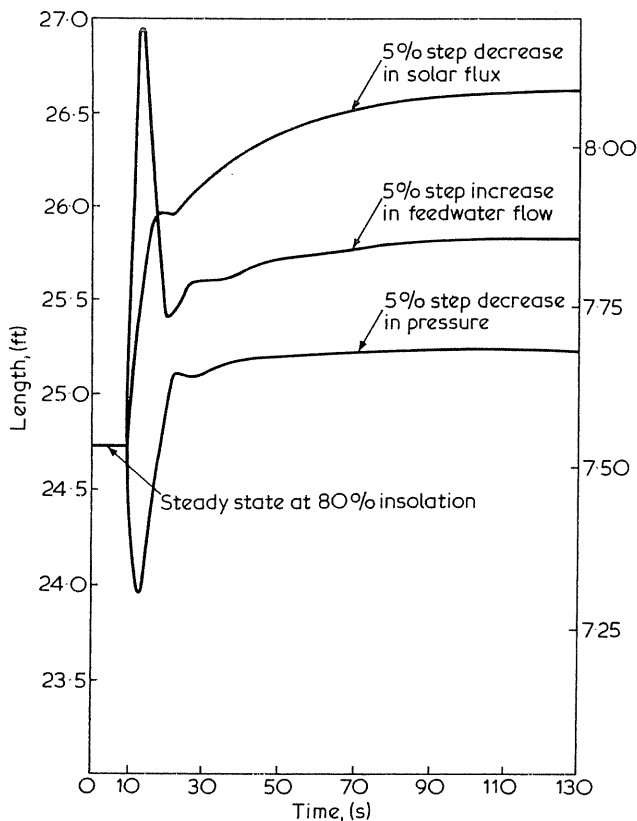


Figure 5 Evaporator length transients at 80% insolation

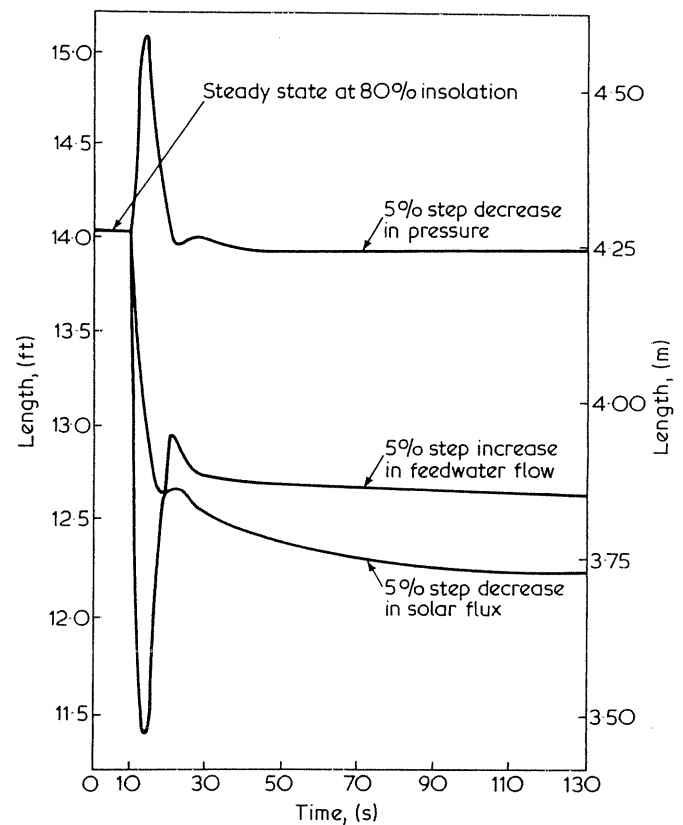


Figure 6 Superheater length transients at 80% insolation

Temperature transients at the steam generator outlet are shown in Figure 3. A reduction in insolation has a delayed effect due to thermal storage in the tube wall. Steam temperature starts declining and then settles down to a steady-state value in about 2 min. An increase in feedwater flow causes steam pressure inside the tube to increase. Since steam enthalpy does not respond so fast, there is an initial rise in steam temperature due to a positive Joule-Thompson coefficient.¹¹ After this small overshoot, temperature decreases rather rapidly and then relaxes to a steady-state in about 90 s. A decrease in steam header pressure results in an initial dip in temperature followed by an overshoot of about 4°C (7°F). Then, temperature monotonically decreases and stabilizes to a lower value. The coupled thermal-hydraulic transient has a response time of about 80 s.

Transient responses of the section lengths (i.e., economizer, evaporator and superheater) are given in Figures 4-6. Decreased insolation reduces heat transfer to water/steam. The lengths of economizer and evaporator increase initially resulting in a decrease in superheater length and, therefore, steam temperature (see Figure 3). Later on, the economizer length stabilizes at a lower value due to a decrease in water/steam pressure at the economizer/evaporator boundary. An increase in feedwater flow results in large initial changes in the length of all three sections due to a fast increase in pressure and, therefore, saturation temperature. After a few oscillations, phase boundaries stabilize with modest increases in economizer and evaporator lengths, and a corresponding decrease in superheater length. Decreased steam header pressure causes abrupt initial decreases in economizer and evaporator lengths and a corresponding increase in superheater length. After a few oscillations, economizer length stabilizes at a lower value due to a reduced water/steam pressure, and the evaporator length at a higher value; the superheater length comes back to almost the original value.

Conclusions

A nonlinear dynamic model of a once-through subcritical steam generator has been derived in state-space form. The model can be used as an element in the overall system simulation of solar thermal plants; it is also suitable for control system design.

By including the temporal acceleration terms in the momentum equations, the model can be extended for flow stability studies in individual steam generator tubes.

References

- 1 Zonderman, K. L. *et al.* In *Preprints AIAA/ASERC Conf. on Solar Energy*, Paper 78-1752, Phoenix, Arizona, 27-29 November 1978
- 2 Durrant, O. W. 'Conceptual design of a solar advanced water/steam receiver', Department of Energy/Sandia Laboratories Central Receiver Semiannual Meeting, Williamsburg, Virginia, USA, 11-12 September 1979
- 3 Ray, A. and Berkowitz, D. A. *J. Dyn. Syst., Measurement Control, Trans. ASME* 1979, **101**, (4), 284
- 4 Berkowitz, D. A. (ed.), 'Proceedings of the seminar on boiler modeling', MITRE Corp., Bedford, Mass., October 1975
- 5 Ray, A. and Bowman, H. F. *J. Dyn. Syst., Measurement Control, Trans. ASME, Ser. G* 1976, **98** (3), 332
- 6 Easton, C. R. *et al.* In *Proc. 9th Inter-Society Energy Conversion Eng. Conf.*, San Francisco, 26-30 August 1974
- 7 Collier, J. G. 'Convective boiling and condensation', McGraw-Hill, London, 1972
- 8 Holman, J. P. 'Heat transfer', McGraw Hill, New York, 1976
- 9 Tong, L. S. 'Boiling heat transfer', Wiley, New York, 1965
- 10 Thaler, G. J. and Pastel, M. P. 'Analysis and design of nonlinear feedback control systems', McGraw Hill, New York, 1962
- 11 Callen, H. B. 'Thermodynamics', Wiley, New York, 1960

Nomenclature

A	tube cross-sectional area for water/steam flow
A_c	convective area on external tube surface per unit length
A_i	inner circumference of tube
A_r	reradiation area on external tube surface per unit length
A_s	effective area for incident solar energy per unit length
C_m	thermal capacity of tube material per unit length
G	mass flow rate of air over external tube surface
g	local acceleration due to gravity
h	specific enthalpy of water/steam
h_{fw}	specific enthalpy of feedwater at tube inlet
K_{cf}	heat transfer constant for forced convection of air
K_{cn}	heat transfer constant for natural convection of air
K_f	constant for frictional pressure drop in water/steam path
K_{mf}	heat transfer constant for water/steam inside tube
k_m	thermal conductivity of tube material
l	length of tube or tube section
P	water/steam pressure
Q	heat transfer rate from external tube surface to water/steam
Q_g	net heat transfer rate from solar collector to external tube surface
r_i	inner tube radius
r_o	outer tube radius
s	Laplace transform variable
T	water/steam temperature
T_a	ambient temperature
T_m	external tube wall temperature

T_0	conversion constant (additive) to absolute temperature
t	time
u	specific internal energy of water/steam
W	mass flow rate of water/steam with respect to tube wall
β	reflectivity of tube wall surface
ϵ	emissivity of external tube surface
ζ, η	state variables for approximation of thermal transport delay
θ	average horizontal inclination of tube helix
ρ	density of water/steam
σ	Stefan-Boltzman constant
τ	thermal transport delay
Ω	solar flux incident on tube surface from heliostats

Appendix

Summary of equation set constituting the mathematical model

The following differential equations identify the selected state variables as $l_{13}, u_2, l_{15}, u_6, \rho_5, T_{m2}, T_{m4}, T_{m6}, \zeta$, and η , respectively:

$$\frac{dl_{13}}{dt} = \left[W_1 - W_3 - \left(\frac{\partial \rho_2}{\partial u_2} \right)_{P_2} (W_1(h_1 - u_2) - W_3(h_3 - u_2) + Q_2) / \rho_2 \right] \times \left[A \left(\rho_2 - \rho_3 + (\rho_3 / \rho_2) \left(\frac{\partial \rho_2}{\partial u_2} \right)_{P_2} (h_3 - u_2) \right) \right]$$

$$\frac{du_2}{dt} = [(W_1(h_1 - u_2) - W_3(h_3 - u_2) + Q_2) / A + \rho_3(h_3 - u_2) dl_{13}/dt] / (\rho_2 l_{13})$$

$$\frac{dl_{15}}{dt} = [\rho_3(h_3 - u_4) dl_{13}/dt - (W_3(h_3 - u_4) - W_5(h_5 - u_4) + Q_4) / A + \rho_4 l_{35} du_4/dt] / (\rho_5(h_5 - u_4))$$

$$\frac{du_6}{dt} = [(W_5(h_5 - u_6) - W_7(h_7 - u_6) + Q_6) / A - \rho_5(h_5 - u_6) dl_{15}/dt] / (\rho_6 l_{57})$$

$$\frac{d\rho_5}{dt} = [(W_3 - W_7) / A + (\rho_5 - \rho_3) dl_{13}/dt] / (l_{35} + l_{57})$$

$$\frac{dT_{m2}}{dt} = (Q_{g2} - Q_2) / (C_m l_{13}) + ((T_{m4} - T_{m2}) / l_{13}) dl_{13}/dt$$

$$\frac{dT_{m4}}{dt} = (Q_{g4} - Q_4) / (C_m l_{35})$$

$$\frac{dT_{m6}}{dt} = (Q_{g6} - Q_6) / (C_m l_{57}) + ((T_{m6} - T_{m4}) / l_{57}) dl_{15}/dt$$

$$\frac{d\zeta}{dt} = \eta - \frac{12}{\tau} h_{fw}$$

$$\frac{d\eta}{dt} = \frac{12}{\tau^2} \zeta - \frac{6}{\tau} \eta + \frac{72}{\tau^2} h_{fw}$$

The supporting algebraic equations are given below:

$$\begin{aligned} P_1 &= P_3 + K_{f2} W_1^2 l_{13} / \rho_2 + \rho_2 g l_{13} \sin \theta \\ W_3 &= \sqrt{(P_3 - P_5 - \rho_4 g l_{35} \sin \theta) \rho_4 / (K_{f4} l_{35})} \\ W_7 &= \sqrt{(P_5 - P_7 - \rho_6 g l_{57} \sin \theta) \rho_6 / (K_{f6} l_{57})} \\ T_{m1} &= 2T_{m2} - T_{m4} \\ T_{m7} &= 2T_{m6} - T_{m4} \\ Q_{g2} &= [A_s \Omega - \sigma \epsilon A_r ((T_{m1} + T_0)^4 + (T_{m4} + T_0)^4) / 2 \\ &\quad - (T_a + T_0)^4] - A_c (K_{cf} G^{0.66} + K_{cn} (T_{m2} - T_a)^{0.33}) \\ &\quad \times (T_{m2} - T_a) l_{13} \\ Q_{g4} &= [A_s \Omega - \sigma \epsilon A_r ((T_{m4} + T_0)^4 - (T_a + T_0)^4) \\ &\quad - A_c (K_{cf} G^{0.66} + K_{cn} (T_{m4} - T_a)^{0.33}) \\ &\quad \times (T_{m4} - T_a) l_{35} \\ Q_{g6} &= [A_s \Omega - \sigma \epsilon A_r ((T_{m4} + T_0)^4 + (T_{m7} + T_0)^4) / 2 \\ &\quad - (T_a + T_0)^4] - A_c (K_{cf} G^{0.66} + K_{cn} (T_{m6} - T_a)^{0.33}) \\ &\quad \times (T_{m6} - T_a) l_{57} \\ Q_2 &= A_i l_{13} (T_{m2} - T_2) / (K_{mf2} W_1^{-0.8} + C_i) \end{aligned}$$

where:

$$\begin{aligned} C_i &= [r_i \ln(r_o/r_i)] / k_m \\ Q_4 &= A_i l_{35} (T_{m4} - T_4) / (K_{mf4} + C_i) \\ Q_6 &= A_i l_{57} (T_{m6} - T_6) / (K_{mf6} W_7^{-0.88} + C_i) \\ h_1 &= \zeta + h_{fw} \\ l_{35} &= l_{15} - l_{13} \\ l_{57} &= l_{17} - l_{15} \end{aligned}$$

where l_{17} = tube length which is a constant.

The following process variables were obtained by thermodynamic relationship and/or averaging interpolation/extrapolation:

$$\begin{aligned} h_5, P_5, T_5 &= f(\rho_5) \\ P_6 &= \text{Ave}(P_5, P_7) \\ \rho_6, h_6, T_6 &= f(u_6, P_6) \\ h_7 &= \text{Ave}(h_5, h_6) \\ T_7 &= f(h_7, P_7) \\ h_2, \rho_2, T_2 &= f(u_2) \\ h_3 &= \text{Ave}(h_1, h_2) \\ P_3, \rho_3, T_3 &= f(h_3) \\ T_4 &= \text{Ave}(T_3, T_5) \\ \rho_4 &= \text{Ave}(\rho_3, \rho_5) \\ h_4 &= \text{Ave}(h_3, h_5) \\ u_4 &= f(h_4, \rho_4) \\ \frac{du_4}{dt} &= \text{Ave} \left(\frac{du_2}{dt}, \left(\frac{\partial u}{\partial \rho} \right)_{\text{Sat. vap.}} \frac{d\rho_5}{dt} \right) \end{aligned}$$

where:

$f()$ indicates a function for thermodynamic state relationship,
 Ave() indicates value obtained by averaging interpolation, and
 Ave() indicates value obtained by averaging extrapolation